Available online at www.sciencedirect.com
SCIENCE DIRECT®
Combustion and Flame 143 (2005) 264–281
Combustion and Flame
www.elsevier.com/locate/combustflame

Effects of H_2 and H preferential diffusion and unity Lewis number on superadiabatic flame temperatures in rich premixed methane flames

Fengshan Liu [a,*], Ömer L. Gülder [b]

[a] *Combustion Technology Group, Institute for Chemical Process and Environmental Technology, National Research Council Canada, Building M-9, 1200 Montreal Road, Ottawa, Ontario, Canada K1A 0R6*
[b] *Institute for Aerospace Studies, University of Toronto, 4925 Dufferin Street, Toronto, Ontario, Canada M3H 5T6*

Received 15 July 2004; received in revised form 20 February 2005; accepted 17 March 2005

Available online 21 July 2005

Abstract

The structures of freely propagating rich CH_4/air and CH_4/O_2 flames were studied numerically using a relatively detailed reaction mechanism. Species diffusion was modeled using five different methods/assumptions to investigate the effects of species diffusion, in particular H_2 and H, on superadiabatic flame temperature. With the preferential diffusion of H_2 and H accounted for, significant amount of H_2 and H produced in the flame front diffuse from the reaction zone to the preheat zone. The preferential diffusion of H_2 from the reaction zone to the preheat zone has negligible effects on the phenomenon of superadiabatic flame temperature in both CH_4/air and CH_4/O_2 flames. It is therefore demonstrated that the superadiabatic flame temperature phenomenon in rich hydrocarbon flames is not due to the preferential diffusion of H_2 from the reaction zone to the preheat zone as recently suggested by Zamashchikov et al. [V.V. Zamashchikov, I.G. Namyatov, V.A. Bunev, V.S. Babkin, Combust. Explosion Shock Waves 40 (2004) 32]. The suppression of the preferential diffusion of H radicals from the reaction zone to the preheat zone drastically reduces the degree of superadiabaticity in rich CH_4/O_2 flames. The preferential diffusion of H radicals plays an important role in the occurrence of superadiabatic flame temperature. The assumption of unity Lewis number for all species leads to the suppression of H radical diffusion from the reaction zone to the preheat zone and significant diffusion of CO_2 from the postflame zone to the reaction zone. Consequently, the degree of superadiabaticity of flame temperature is also significantly reduced. Through reaction flux analyses and numerical experiments, the chemical nature of the superadiabatic flame temperature phenomenon in rich CH_4/air and CH_4/O_2 flames was identified to be the relative scarcity of H radical, which leads to overshoot of H_2O and CH_2CO in CH_4/air flames and overshoot of H_2O in CH_4/O_2 flames.

Keywords: Rich premixed flames; Preferential diffusion; Superadiabatic flame temperature; Chemical kinetics; Chemical equilibrium

1. Introduction

The phenomenon of superadiabatic flame temperature (SAFT) in rich hydrocarbon premixed flames

* Corresponding author. Fax: +1 613 957 7869.
E-mail address: fengshan.liu@nrc-cnrc.gc.ca (F. Liu).

0010-2180/$ – see front matter
doi:10.1016/j.combustflame.2005.03.018

is of great fundamental and practical interest. It has been observed experimentally and predicted numerically [1–6]. In a numerical study of diamond chemical vapor deposition (CVD) using a strained, rich premixed $C_2H_2/H_2/O_2$ flame, Meeks et al. [1] found that the flame temperature exceeds the adiabatic temperature, which is somewhat unusual in premixed hydrocarbon flames. Their study is perhaps the first numerical work to reveal the phenomenon of SAFT in rich premixed hydrocarbon flames. The appearance of superadiabatic temperature in the flame numerically studied by Meeks et al. [1] was subsequently confirmed experimentally by Bertagnolli and Lucht [2] and Bertagnolli et al. [3]. Meeks et al. [1] suggested that the primary reason for the occurrence of SAFT in the rich $C_2H_2/H_2/O_2$ premixed flame is that unreacted acetylene requires a relatively long time to dissociate to its equilibrium concentration. Another explanation of SAFT in this flame was later presented by Bertagnolli et al. [3], who believed that the presence of superequilibrium concentrations of CO_2 and H_2O was the primary cause of the superadiabatic flame temperatures. The superequilibrium concentrations of C_2H_2 and H_2O are consistent with the subequilibrium concentrations of H and H_2. Later in a numerical study of CVD of diamond films using rich acetylene–oxygen flames, Ruf et al. [4] also noted the significantly subequilibrium concentration of H and suggested that the slow and endothermic reaction $H_2 + M \Leftrightarrow H + H + M$ is responsible for the subequilibrium concentration of H and SAFT. More recently, the nature of SAFT has been explored by Liu et al. [5] and Zamashchikov et al. [6] in their numerical studies of freely propagating rich hydrocarbon premixed flames. Through a systematic investigation of the structure and maximum flame temperature in CH_4/air, CH_4/O_2, $C_2H_2/H_2/O_2$, C_2H_4/O_2, C_3H_8/O_2, and H_2/O_2 flames, Liu et al. [5] found that SAFT occurs only in rich hydrocarbon flames but not in hydrogen flames and suggested that the nature of SAFT is chemical kinetics. However, Zamashchikov et al. [6] concluded, through a careful examination of the numerically predicted structures of rich C_3H_8/air and CH_4/air flames, that the nature of SAFT in rich hydrocarbon flames is the diffusion of molecular hydrogen from the reaction zone to the preheat zone and its preferential oxidation compared to hydrocarbons. While the superadiabatic flame temperature phenomenon is clearly a nonequilibrium process, the brief review of the literature discussed above on this topic reveals that our current understanding of the nature of SAFT remains unclear given the two completely different views presented in Refs. [5,6].

Although it has been made clear that the mechanism of superadiabatic temperature in diffusion flames, such as the numerical study of Takagi and Xu [7], is a direct consequence of the preferential diffusion effects of H_2 and H, the effects of preferential diffusion of H_2 and H and the Lewis number in general on the occurrence of SAFT in rich hydrocarbon premixed flames have yet to be explored. This study is motivated by the lack of understanding of the effects of preferential diffusion of H_2 and H and the species Lewis number on SAFT in rich premixed hydrocarbon flames. Although the nature of SAFT was previously speculated to be chemical kinetics [1,3–5], the question of why SAFT occurs when a hydrocarbon mixture is sufficiently rich has not been adequately answered. An attempt was also made in this study to provide further insight into the nature of SAFT. In the present study, the structures of atmospheric freely propagating planar rich premixed flames in mixtures of CH_4/air and CH_4/O_2 were numerically computed using detailed chemistry and complex thermal and transport properties. To investigate the effects of preferential diffusion of H_2 and H from the reaction zone to the preheat zone and the Lewis number on SAFT, numerical calculations were carried out using five different treatments of species diffusion. Reaction flux analyses were performed to reveal the chemical nature of SAFT.

2. Numerical model

The conservation equations of mass, momentum, energy, and chemical species for steady planar freely propagating premixed flames were solved using a CHEMKIN-based code [8]. The thermochemical and transport properties of species were obtained from CHEMKIN [8] and TPLIB [9,10] database. Since our previous study found that radiation heat loss has negligible impact on the flame temperature in the reaction zone and the immediate postflame zone [5], all the calculations were conducted without radiation heat loss. At a spatial location of $x = 0.05$ cm, the mixture temperature is fixed at 400 K. In all the calculations, the upstream location (fresh mixture) is always kept at $x = -2.5$ cm. The location of downstream (reacted combustion products) specified in the calculations varies with the gas mixture. In all the calculations, however, it was checked that the computational domain was sufficiently long to achieve adiabatic equilibrium. The gas mixture temperature at the upstream boundary was kept at 300 K and zero-gradient conditions were specified at the downstream boundary. All the calculations were performed at atmospheric pressure. The GRI Mech 3.0 reaction mechanism [11], which was optimized for methane combustion, was used to model the chemical kinetics in this work. The only modification made to this mechanism is the re-

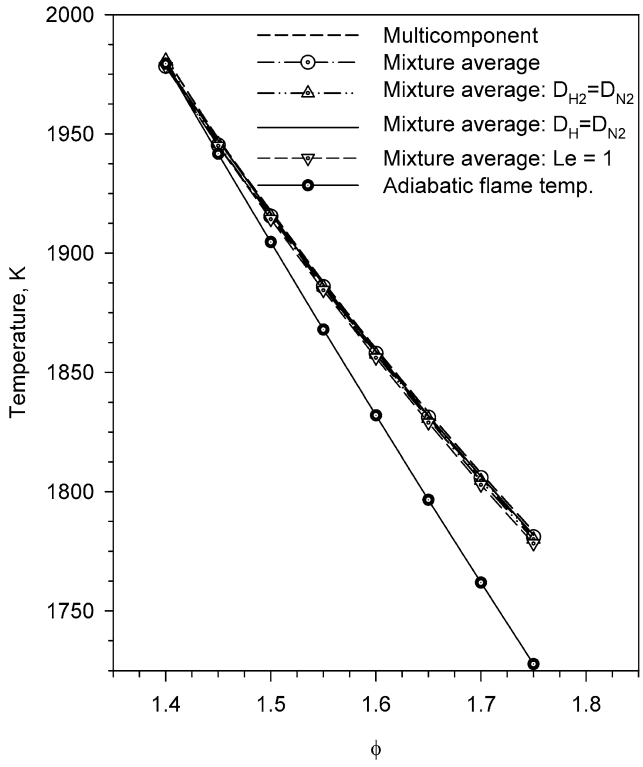

Fig. 1. Variation of the maximum flame temperature with the equivalence ratio in rich CH_4/air mixtures.

moval of species (except N_2) and reactions related to NO_x formation. To investigate the effects of preferential diffusion of H_2 and H from the reaction zone to the preheat zone and the Lewis number on SAFT, calculations were conducted using the following five treatments of species diffusion: (1) multicomponent formulism, (2) mixture-averaged formulism, (3) mixture average with the assumption that H_2 has the same diffusion coefficient as N_2, (4) mixture average with the assumption that H has the same diffusion coefficient as N_2, and (5) mixture average with the assumption of unity Lewis number for all species. The former two are the usual species diffusion models available in CHEMKIN codes [8]. The latter three were implemented under the *mixture-averaged formulism* for species diffusion by further imposing one of the following three constraints: (i) the diffusion coefficient of H_2 is equal to that of N_2, i.e., $D_{H_2} = D_{N_2}$, (ii) the diffusion coefficient of H is equal to that of N_2, i.e., $D_H = D_{N_2}$, and (iii) unity Lewis number for all species, i.e., $D_K = \lambda/\rho c_p$, with λ being the mixture thermal conductivity, ρ the mixture density, and c_p the mixture specific heat. Thermal diffusion of H_2 and H was taken into account only in the first species diffusion model, i.e., the multicomponent formulism.

3. Results and discussion

3.1. Effect of preferential diffusion in methane/air flames

Methane/air flames were calculated for equivalence ratios (ϕ) between 1.4 and 1.75. Fig. 1 shows the variation of the maximum flame temperatures calculated using the five species diffusion models and the adiabatic equilibrium temperature with the equivalence ratio. At $\phi = 1.4$, the adiabatic equilibrium temperature is essentially the same as the maximum flame temperatures; i.e., SAFT does not occur. As the equivalence ratio increases, the maximum flame temperatures start to exceed the adiabatic flame temperature and the degree of superadiabaticity also increases with ϕ. At $\phi = 1.75$, the maximum flame temperatures exceed the adiabatic equilibrium one by about 50 to 56 K, depending on the diffusion model. It has been previously found by Liu et al. [5] that SAFT occurs in premixed hydrocarbon flames only when the equivalence ratio exceeds a critical value. Results shown in Fig. 1 are also qualitatively similar to those obtained by Zamashchikov et al. [6] in C_3H_8/air flames. It has been shown previously that the occurrence of superadiabatic temperature is associated with negative heat release rates in the immediate postflame

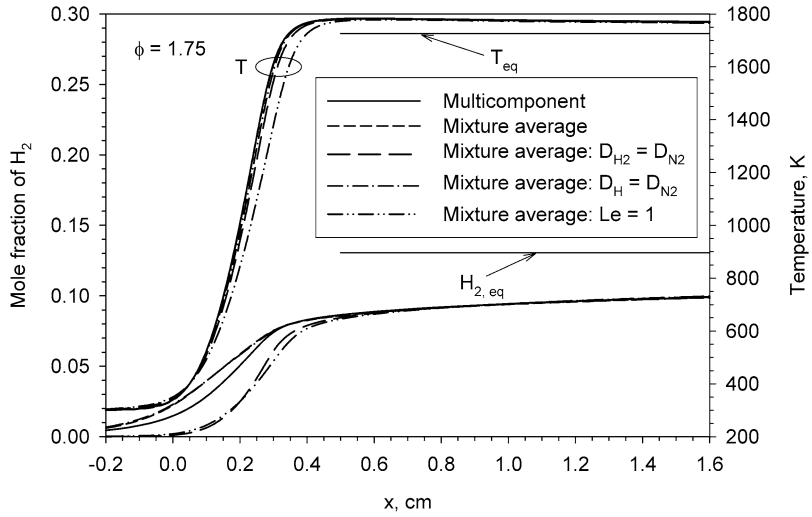

Fig. 2. Spatial distributions of the mole fraction of H_2 and temperature in a rich CH_4/air flame of $\phi = 1.75$.

region [5]. Results displayed in Fig. 1 indicate that the maximum flame temperature in rich CH_4/air mixtures always exceeds the adiabatic equilibrium value when the equivalence ratio is greater than 1.4, regardless of how the species diffusion is calculated. In addition, the differences between the maximum temperatures calculated using the five species diffusion models are quite small. In other words, the effects of preferential diffusion of H_2 and H from the reaction zone to the preheat zone and the Lewis number on the maximum flame temperature are insignificant in these CH_4/air flames. It is somewhat surprising to observe from Fig. 1 that SAFT always occurs regardless of the treatment of species diffusion, given the recent study by Zamashchikov et al. [6] who concluded that the nature of SAFT is H_2 diffusion from the reaction zone to the preheat zone. Results shown in Fig. 1 provide the first direct numerical evidence that SAFT occurs in rich CH_4/air flame even when the preferential diffusion of H_2 from the reaction zone to the preheat zone is artificially suppressed (see Fig. 2). These results clearly demonstrate that the nature of SAFT is not H_2 diffusion from the reaction zone to the preheat zone, contrary to the claim recently made by Zamashchikov et al. [6].

To illustrate the effects of the five species diffusion models on the calculated flame structure, the spatial distributions of temperature and H_2 mole fractions for the richest mixture considered, i.e., $\phi = 1.75$, are compared in Fig. 2. Indeed there is a significant amount of H_2 diffused from the reaction zone, roughly between $x = 0.25$ and 0.4 cm, to the preheat zone, between $x = 0.05$ and 0.25 cm, when the species diffusion models 1, 2, and 4 were used in the calculations. Although there is some quantitative difference in the H_2 mole fraction profile between the results of species diffusion models 1 and 2, the corresponding temperature profiles are almost identical, implying that the mixture-averaged formulism diffusion model is adequate in the calculations of CH_4/air mixtures. The significant diffusion of H_2 from the reaction zone to the preheat zone is expected, since H_2 has a much higher diffusion coefficient than other species. When the species diffusion models 3 and 5 were used, however, preferential diffusion of H_2 from the reaction zone to the preheat zone is effectively suppressed. In this mixture, while the temperature in the postflame region stays above the adiabatic equilibrium value, the mole fraction of H_2 remains substantially below its equilibrium value even at $x = 1.6$ cm. In fact, adiabatic equilibrium in this mixture is reached at a location of about $x = 170$ cm. The temperature profiles shown in Fig. 2 indicate that (i) SAFT always occurs regardless of how species diffusion is calculated, with or without preferential diffusion of H_2 and/or H, and (ii) the assumption of unity Lewis number for all species leads to the slowest rise in the temperature in the reaction zone. The slow rise in the flame temperature under the diffusion model 5 can be attributed to the chemically inhibiting effect of CO_2, which is diffused from the postflame region to the reaction zone as a result of an enhanced diffusion coefficient for CO_2, through competition for H radicals via the reverse reaction of $CO + OH \Leftrightarrow CO_2 + H$ (R99) [12].

The spatial distributions of mole fractions of O, OH, H, and HO_2 radicals in the $\phi = 1.75$ flame are shown in Fig. 3. Overall the mole fractions of O, OH, and H radicals are quite low in this flame where the flame temperature is also relatively low (below 1800 K), especially for O and OH. It is evident that the mole fractions of O, OH, and H substantially ex-

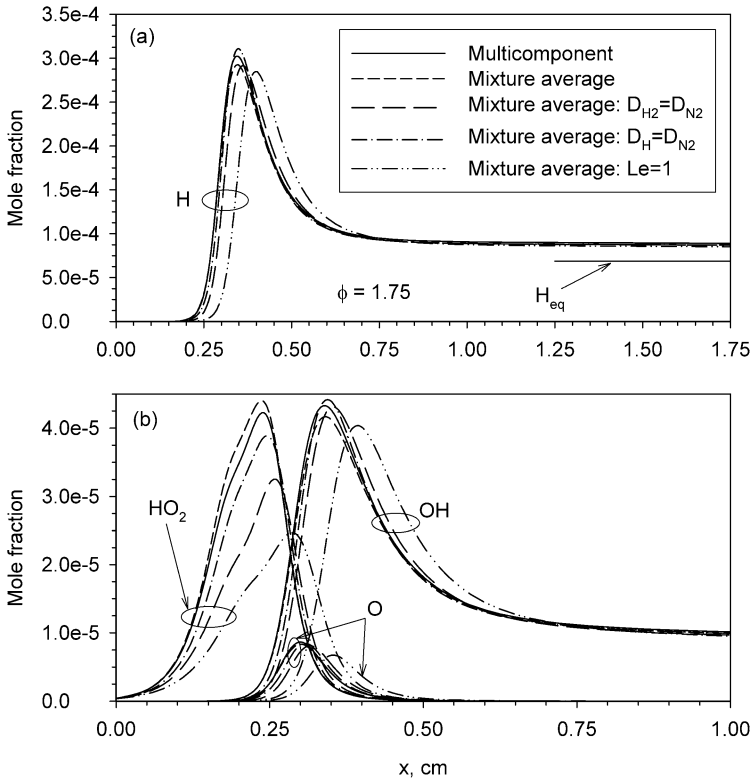

Fig. 3. Spatial distributions of the mole fraction of O, OH, H, and HO_2 radicals in a rich CH_4/air flame of $\phi = 1.75$.

ceed their equilibrium values in this flame, especially the H radical with its peak values about four times that of the equilibrium value. The overshoot of these radical concentrations in premixed hydrocarbon/air flames is well known and is a consequence of fast two-body radical-generating reactions in the reaction zone followed by slow three-body recombination reactions as the system proceeds to equilibrium. Unlike the diffused H_2 from the reaction zone to the preheat zone that can survive in significant amounts in the preheat zone, especially the results of diffusion models 1, 2, and 4 in Fig. 2, H radicals cannot survive in substantial amounts in the preheat zone; even the preferential diffusion of H is allowed in species diffusion models 1, 2, and 3. A possible reason for this is that H radicals preferentially diffused from the reaction zone to the preheat zone are rapidly consumed by reactions $H + O_2 + M \Leftrightarrow HO_2 + M$ (R33), $H + O_2 + H_2O \Leftrightarrow HO_2 + H_2O$ (R35), and $H + O_2 + N_2 \Leftrightarrow HO_2 + N_2$ (R36) to form HO_2, $H + CH_4 \Leftrightarrow CH_3 + H_2$ (R53), $H + O_2 \Leftrightarrow O + OH$ (R38), and $H + CH_2O \Leftrightarrow HCO + H_2$ (R58). The insignificant effect of H radical preferential diffusion on its mole fraction distribution across the reaction zone shown in Fig. 3a may be attributed to the following two factors: (i) the H radical concentration is quite low, and (ii) the flame thickness is fairly large, leading to a relatively small concentration gradient. Once again it is seen that assumption of unity Lewis number for all species, diffusion model 5, has the most significant influence on the mole fractions of these radicals, which primarily delays the reactions and secondly reduces the mole fractions of these radicals, due to the chemically inhibiting effect of CO_2 noted earlier. Nevertheless, preferential diffusion affects the H_2 concentration distribution significantly but only moderately the H radical concentration in rich CH_4/air flames.

The spatial distributions of mole fractions of major species O_2, CH_4, H_2O, CO, and CO_2 are compared in Fig. 4. With the exception that the mole fraction of O_2 rapidly decays to its equilibrium value, the mole fractions of H_2O, CO_2, and CH_4 exceed their equilibrium values in the postflame region, especially H_2O, while the mole fraction of CO, like H_2 shown in Fig. 2, remains substantially below its equilibrium value. The primary pathways for the decay of mole fractions of CO_2 and H_2O to their equilibrium values in the postflame region are the reverse reactions of $OH + CO \Leftrightarrow H + CO_2$ (R99) and $OH + H_2 \Leftrightarrow H + H_2O$ (R84). As the mole fractions of CO_2 and H_2O decay to their equilibrium values through these two reactions, the mole fractions of CO and H_2 are increased to their respective equilibrium values, consistent with subequilibrium mole fractions of H_2 and CO in the immediate

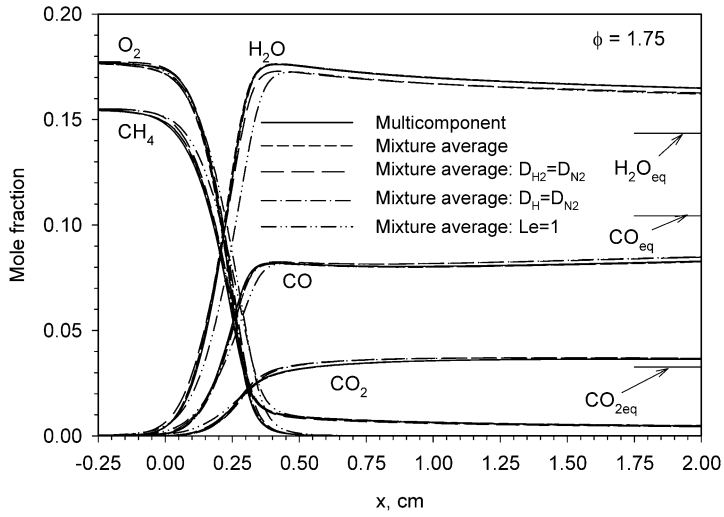

Fig. 4. Spatial distributions of the mole fraction of major species O_2, CH_4, CO, CO_2, and H_2O in a rich CH_4/air flame of $\phi = 1.75$.

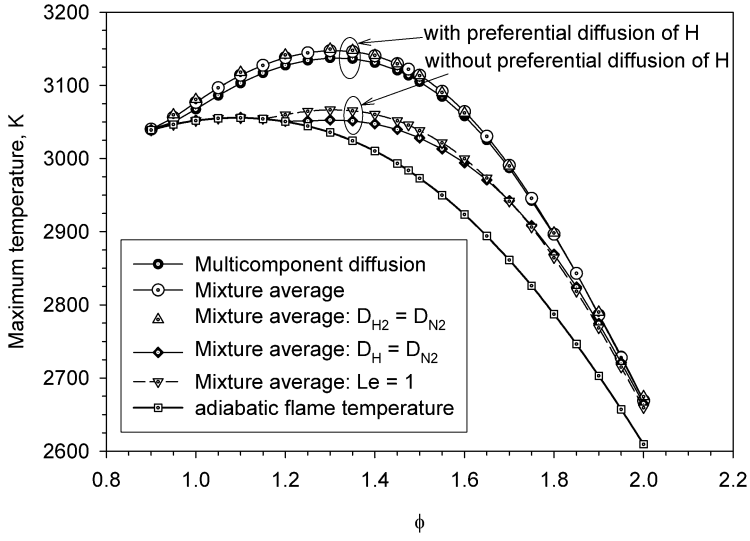

Fig. 5. Variation of the maximum flame temperature with the equivalence ratio in rich CH_4/O_2 mixtures.

postflame region shown in Figs. 2 and 4. It is also evident from the mole fraction profiles of these major species that the assumption of unity Lewis number leads to delayed chemical reactions. The enhanced diffusion of CO_2 from the postflame region to the reaction zone is clearly seen from the spatial distribution of CO_2 mole fraction.

In summary, the numerical results demonstrate that preferential diffusion of H_2 and H only insignificantly affects the overall flame structure and the degree of temperature overshoot. The assumption of unity Lewis number for all species has a larger impact on the calculated flame structure than the preferential diffusion of H_2 or H alone. However, none of the five species diffusion models qualitatively alters the flame structure or the occurrence of SAFT in rich CH_4/air flames.

3.2. Effect of preferential diffusion in methane/oxygen flames

The structure of CH_4/O_2 flames was computed for a series of equivalence ratios between 0.9 and 2 using the five species diffusion models. Variations of the maximum flame temperature with ϕ are compared in Fig. 5. It is first observed that SAFT occurs only when the equivalence ratio ϕ is larger than 0.9 in CH_4/O_2 mixtures, as indicated by the results of the first two

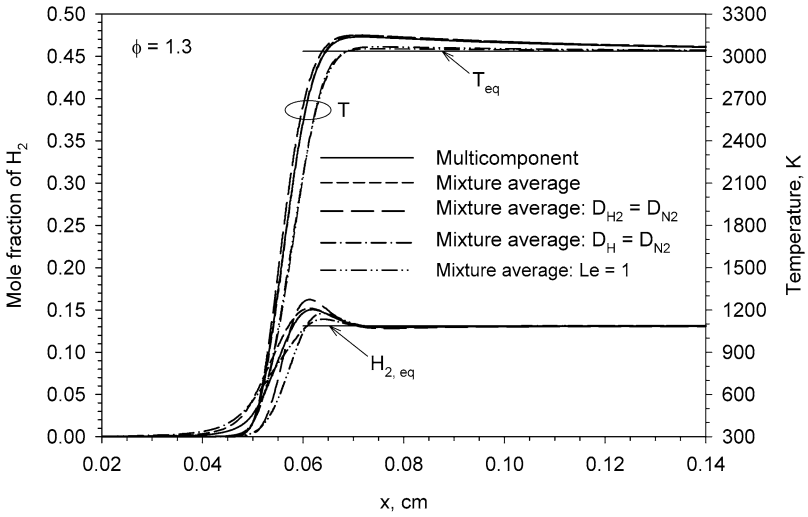

Fig. 6. Spatial distributions of the mole fraction of H_2 and temperature in a rich CH_4/O_2 flame of $\phi = 1.3$.

diffusion models. The degree of superadiabaticity (the difference between the maximum temperature based on the multicomponent formulism and the adiabatic flame temperature) first increases with ϕ until about $\phi = 1.55$, where the maximum temperature exceeds the adiabatic flame value by about 134 K, and then gradually decreases with further increase in ϕ. In such mixtures, use of the mixture-averaged formulation for species diffusion predicts the maximum flame temperatures that are only slightly higher than those based on the multicomponent formulism and the difference vanishes as ϕ increases beyond 1.6. Similar to the results for CH_4/air mixtures, the suppression of preferential diffusion of H_2 from the reaction zone to the preheat zone by assuming $D_{H_2} = D_{N_2}$, diffusion model 3, has a negligible impact on the maximum flame temperatures and therefore does not affect the phenomenon of SAFT. However, it is very interesting to observe from Fig. 5 that the suppression of the preferential diffusion of H radicals from the reaction zone to the preheat zone, using diffusion models 4 and 5, significantly reduces the degree of superadiabaticity in CH_4/O_2 mixtures. In fact, SAFT is almost completely eliminated for CH_4/O_2 mixtures between $\phi = 0.9$ and $\phi = 1.15$ when the preferential diffusion of the H radical is suppressed. These results are very different from those of CH_4/air mixtures where the preferential diffusion of H radicals has only a small influence on the maximum flame temperatures shown in Fig. 1. While the elimination of the preferential diffusion of H radicals, diffusion models 4 and 5, significantly reduces the maximum flame temperatures for equivalence ratios between 0.9 and about 1.7, its effect gradually vanishes as the equivalence ratio further increases. Once again the results shown in Fig. 5 demonstrate that the nature of SAFT is not the preferential diffusion of H_2 from the reaction zone to the preheat zone as claimed by Zamashchikov et al. [6], since SAFT always occurs with or without the preferential diffusion of H_2 and/or H.

To examine the effects of species diffusion models on the structure of the flame, the temperature and H_2 mole fraction profiles calculated for $\phi = 1.3$ are compared in Fig. 6. Once again we can see that a significant amount of H_2 present in the preheat zone (roughly between $x = 0.04$ cm and $x = 0.055$ cm) when species diffusion models 1, 2, and 4 were used in the calculations is a result of preferential diffusion of H_2 from the reaction zone. Similar to the results shown in Fig. 2, the preferential diffusion of H_2 from the reaction zone to the preheat zone is effectively suppressed when species diffusion models 3 and 5 were employed in the calculations. Unlike the H_2 mole fraction profile in the CH_4/air flame shown in Fig. 2, where the mole fraction of H_2 remains substantially below its equilibrium value, the mole fraction of H_2 first exceeds its equilibrium value in the reaction zone and then rapidly decays to the equilibrium level. It is evident from the temperature profiles shown in Fig. 6 that SAFT occurs in this mixture regardless of how the species diffusion is calculated; i.e., SAFT occurs even when the preferential diffusion of H_2 or H is eliminated. Temperature profiles shown in both Figs. 2 and 6 indicate that the assumption of unity Lewis number for all species has the most significant impact on reducing the degree of superadiabaticity and the temperature gradient in the flame front (associated with the burning velocity), especially in CH_4/O_2 flames. It is interesting to observe from Fig. 6 that the degree of superadiabaticity correlates well with the combustion intensity (characterized by the slope of temperature rise in the

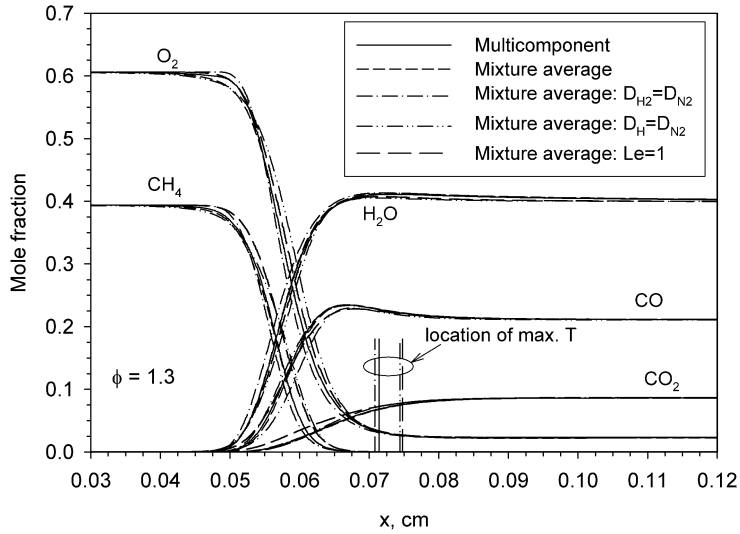

Fig. 7. Spatial distributions of the mole fraction of major species O_2, CH_4, CO, CO_2, and H_2O in a rich CH_4/O_2 flame of $\phi = 1.3$.

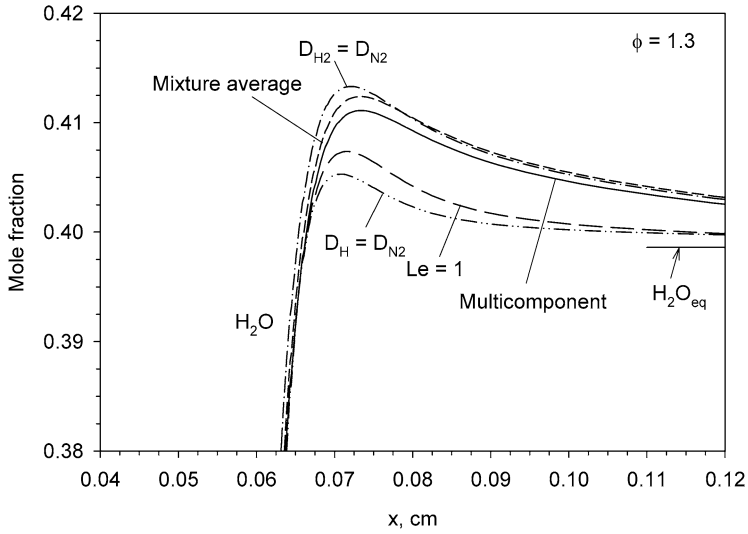

Fig. 8. Spatial distributions of the mole fraction of H_2O in the immediate postflame region in a rich CH_4/O_2 flame of $\phi = 1.3$.

flame front): the stronger the combustion intensity, the larger the temperature overshoot.

To gain further insight into the effects of species diffusion on the flame structure, spatial distributions of mole fraction of major species and three important radicals (O, H, and OH) calculated for $\phi = 1.3$ are shown in Figs. 7–9. Also plotted in these figures are the locations of the maximum temperature corresponding to each species diffusion model. The first two species diffusion models yield identical locations of the maximum temperature. Overall it can be observed that results of the first two species diffusion models (multicomponent and mixture average formulism) are in very good agreement, especially for CO, CO_2, H_2O, and the three radicals. On the other hand, the latter three species diffusion models have rather significant effects on the calculated species mole fraction profiles, especially the assumption of unity Lewis number. In contrast to rich CH_4/air flames where the two intermediate species CO and H_2 remain subequilibrium in the reaction zone (Figs. 2 and 4) their mole fractions exceed the respective equilibrium values in the reaction zone in rich CH_4/O_2 flames (Figs. 6 and 7). It is interesting to note that there is substantial amount of O_2 survived in the equilibrium product even though this is a rich mixture. The earlier decay in the mole fraction profiles of CH_4 and O_2 between about $x = 0.04$ and

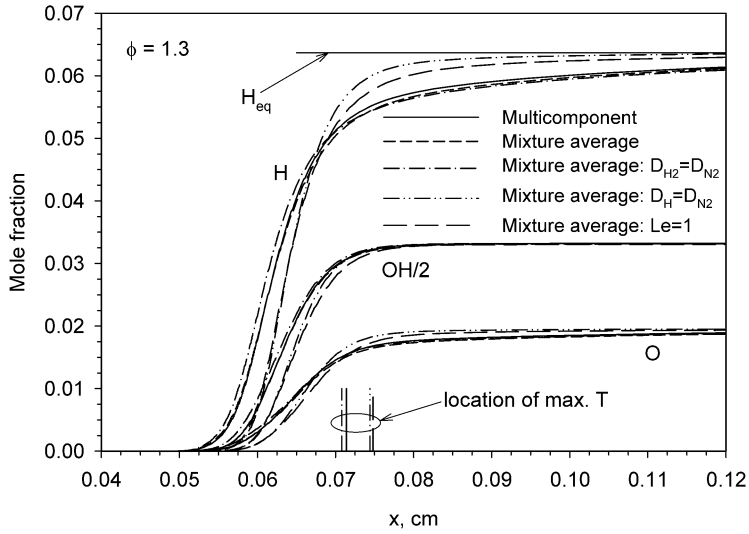

Fig. 9. Spatial distributions of the mole fraction of O, OH, and H radicals in a rich CH_4/O_2 flame of $\phi = 1.3$.

0.05 cm when using species diffusion models 1, 2, and 4 is not due to chemical reactions, but attributed to the increase in the total number of moles due to the supply of H_2 and/or H preferentially diffused from the reaction zone to this region. Regardless of how species diffusion was calculated, the degree of temperature overshoot is directly related to the degree of H_2O overshoot (Figs. 5 and 8). Relative to the results of the first two species diffusion models, it is interesting to note that the assumption of $D_{H_2} = D_{N_2}$ enhances combustion, as evidenced by the earlier and faster rise in the temperature shown in Fig. 6 and in H radical mole fractions shown in Fig. 9. In addition, the elimination of H_2 preferential diffusion alone, species diffusion model 3, even slightly increases the degree of superadiabaticity for equivalence ratios between 0.95 and 1.35 shown in Fig. 5. These effects of the elimination of the preferential diffusion of H_2 alone in CH_4/O_2 mixtures were not observed in the CH_4/air mixtures. The enhanced combustion when using species diffusion model 3 may be explained by the concentrations of H_2 and H in the early stage of fuel breakup through the most important fuel consumption step $H + CH_4 \Leftrightarrow CH_3 + H_2$ (R53). Use of the species diffusion model 3 eliminates the preferential diffusion of H_2 from the reaction zone to the preheat zone, but still permits the preferential diffusion of H radicals. As such, the net reaction rate of R53 is larger than that of using diffusion models 1 or 2, therefore enhancing the overall combustion intensity. The absence of these effects of the species diffusion model 3 in the CH_4/air mixtures may be attributed to the much lower mole fraction of H radicals and much lower temperatures. The substantially inhibited combustion as a result of eliminating the preferential diffusion of H radicals, as evidenced by the slow rise in the temperature shown in Fig. 6, can also be explained in terms of the important role of H radicals in the fuel consumption step R53. The almost identical temperature profiles calculated using diffusion models 4 and 5 imply that the elimination of H radical preferential diffusion plays the most important role in reducing the combustion intensity in this mixture, while the inhibiting effect of CO_2 diffused from the postflame zone to the reaction zone when using diffusion model 5 in this case is relatively small due to the abundance in H radicals.

The spatial distributions of mole fractions of O, OH, and H radicals in the CH_4/O_2 mixture shown in Fig. 9 are radically different from those shown in Fig. 3 in the CH_4/air mixture. First, the mole fractions of these radicals are subequilibrium in the CH_4/O_2 mixture, but substantially exceed their equilibrium values in the CH_4/air mixture. Secondly, the mole fractions of these radicals in the CH_4/O_2 mixture are higher than those in the CH_4/air mixture by two to three orders of magnitude. Thirdly, the spatial profiles of H mole fractions exhibit significant differences between results with and without the preferential diffusion of H radicals in the preheat zone, the reaction zone, and the postflame zone. The elimination of the preferential diffusion of the H radical, diffusion models 4 and 5, leads to a much delayed but sharper rise in the mole fraction of the H radical to its equilibrium value. The much faster approach of the H radical to its equilibrium value with the elimination of H radical preferential diffusion is closely associated with the reduced degree of superadiabaticity in this mixture shown in Figs. 5 and 6.

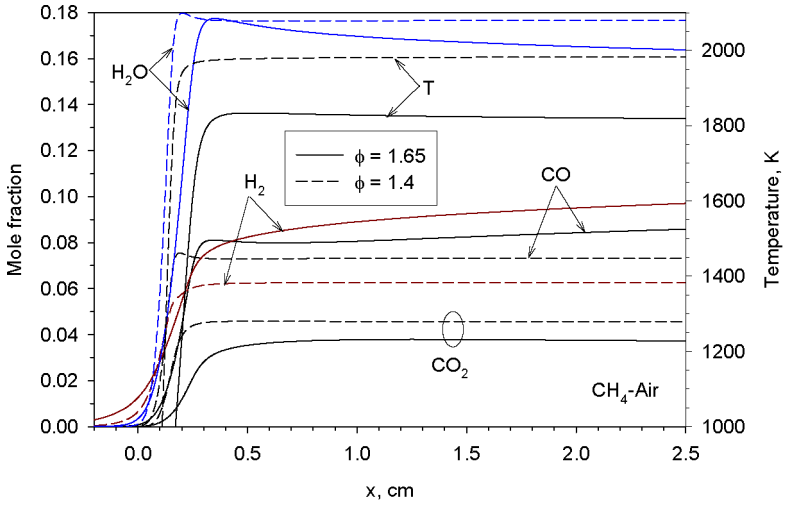

Fig. 10. Spatial distributions of T, CO, CO_2, H_2, and H_2O in two CH_4/air flames of $\phi = 1.65$ and 1.4.

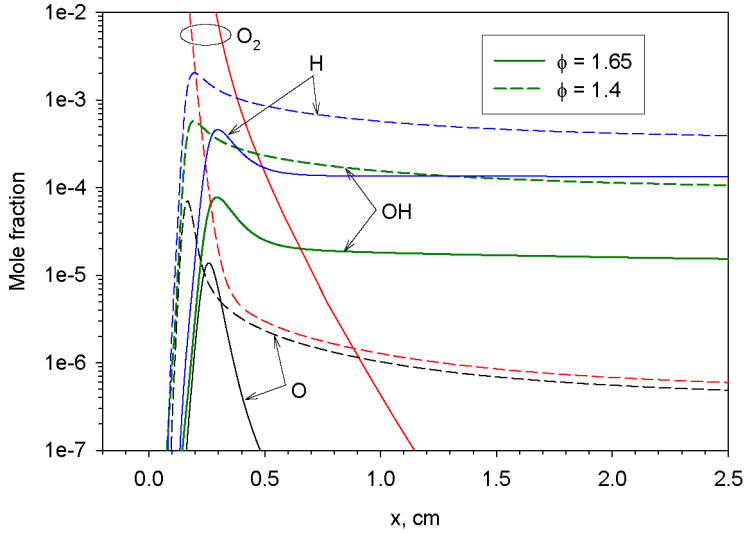

Fig. 11. Spatial distributions of O_2, H, OH, and O in two CH_4/air flames of $\phi = 1.65$ and 1.4.

The numerical results obtained for CH_4/O_2 flames again demonstrate that the nature of SAFT is not preferential diffusion of H_2 molecules. Instead, the results shown in Figs. 5 and 6 reveal that the preferential diffusion of H radicals significantly enhances the level of SAFT in CH_4/O_2 flames. However, suppression of H radical preferential diffusion cannot eliminate the occurrence of SAFT.

3.3. *Chemical kinetics nature of SAFT*

The numerical results discussed above indicate that the nature of SAFT is *not* species preferential diffusion. Although the nature of SAFT was suggested to be chemical kinetics [1,3–5], there is still lack of adequate understanding on the specifics of kinetics responsible for the occurrence of SAFT. In this section, the chemical kinetics in rich CH_4/air and CH_4/O_2 flames was examined through reaction flux analysis to gain insight into the nature of SAFT. The chemical kinetics in rich CH_4/air flames is first discussed. The numerical results discussed in this section were obtained using the first method for modeling species diffusion.

As shown in Fig. 1, SAFT occurs in CH_4/air flames only when the equivalence ratio is greater than 1.4. To understand how such particularity of rich CH_4/air flames, i.e., the SAFT phenomenon, depends on the equivalence ratio, the flame structure of $\phi = 1.65$ is compared with that of $\phi = 1.4$ in Figs. 10–12. As the equivalence ratio increases, a clear change in the flame structure can be observed: (1) the

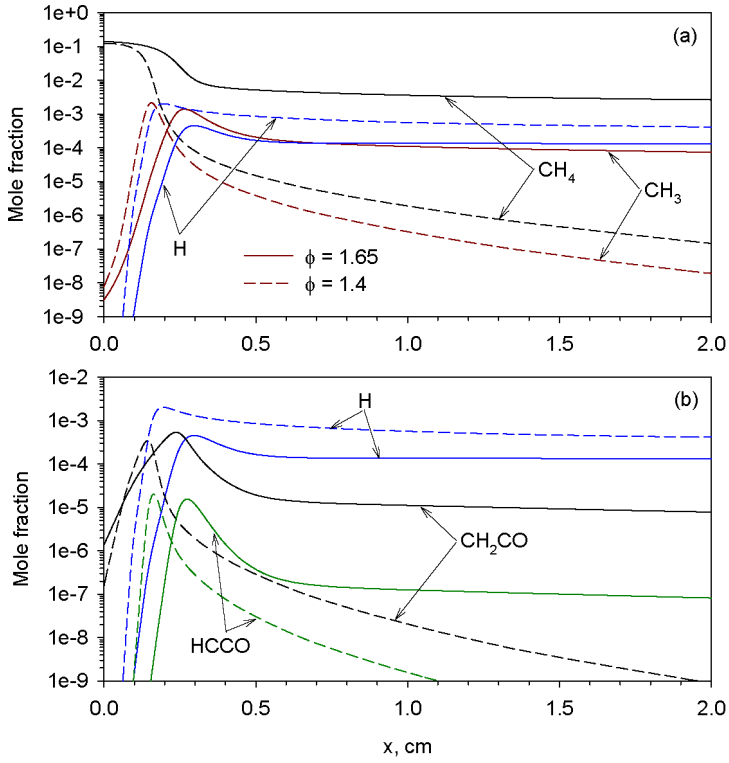

Fig. 12. Spatial distributions of H, CH_4, CH_3, HCCO, and CH_2CO in two CH_4/air flames of $\phi = 1.65$ and 1.4.

flame temperature decreases, (2) concentrations of the two intermediate species CO and H_2 increase, especially H_2, while the two stable product species CO_2 and H_2O decrease (Fig. 10), (3) concentrations of the three radicals O, OH, and H decrease (Fig. 11), and (4) concentrations of hydrocarbons species, such as CH_4, CH_3, HCCO, and CH_2CO, increase substantially (Fig. 12). These differences are the direct consequence of increasingly incomplete oxidation of intermediate species with increasing the equivalence ratio. For the flame of $\phi = 1.4$, the mole fraction of H_2O at the flame front only slightly exceeds its equilibrium value and then decays rapidly to the equilibrium level. In contrast, the mole fraction of H_2O in the flame of $\phi = 1.65$ not only more significantly exceeds its equilibrium value but also decays much more slowly to the equilibrium concentration (Fig. 10). This difference in the mole fraction of H_2O in the postflame region is governed by reaction $OH + H_2 \Leftrightarrow H + H_2O$ (R84) whose heat release rates in these two flames are compared in Fig. 13, which displays the major heat release reactions. Fig. 13 shows that R84 first proceeds forward and then backward in both flames. In the flame of $\phi = 1.4$ the reverse reaction of R84 takes place only briefly before it reaches equilibrium. In this flame, the net heat release rate approaches zero monotonically from positive values (Fig. 13b) implying no occurrence of SAFT. In the richer flames of $\phi = 1.65$, however, the reverse reaction of R84 lasts much longer; i.e., the recovery to equilibrium is very slow, and the net heat release rate at the postflame region first drops below zero and then slowly approaches zero (Fig. 13a).

To identify reactions responsible for the endothermicity in the postflame region Fig. 14a displays the major endothermic reactions in this region in the flame of $\phi = 1.65$. The major endothermic reactions are

$$CH_2 + CO + (M) \Leftrightarrow CH_2CO + (M), \quad \text{(R140)}$$

$$OH + H_2 \Leftrightarrow H_2O + H, \quad \text{(R84)}$$

$$H + C_2H_2 + (M) \Leftrightarrow C_2H_3 + (M), \quad \text{(R71)}$$

$$H + C_2H_4 + (M) \Leftrightarrow C_2H_5 + (M), \quad \text{(R74)}$$

$$H + CH_2O + (M) \Leftrightarrow CH_2OH + (M), \quad \text{(R56)}$$

$$H + O_2 \Leftrightarrow O + OH. \quad \text{(R38)}$$

Among these reactions, the first two reactions (dissociation of CH_2CO and H_2O via R140 and R84, respectively) contribute the most to the endothermicity in this flame in the postflame region. It is worth pointing out that, except for the dissociation of CH_2CO

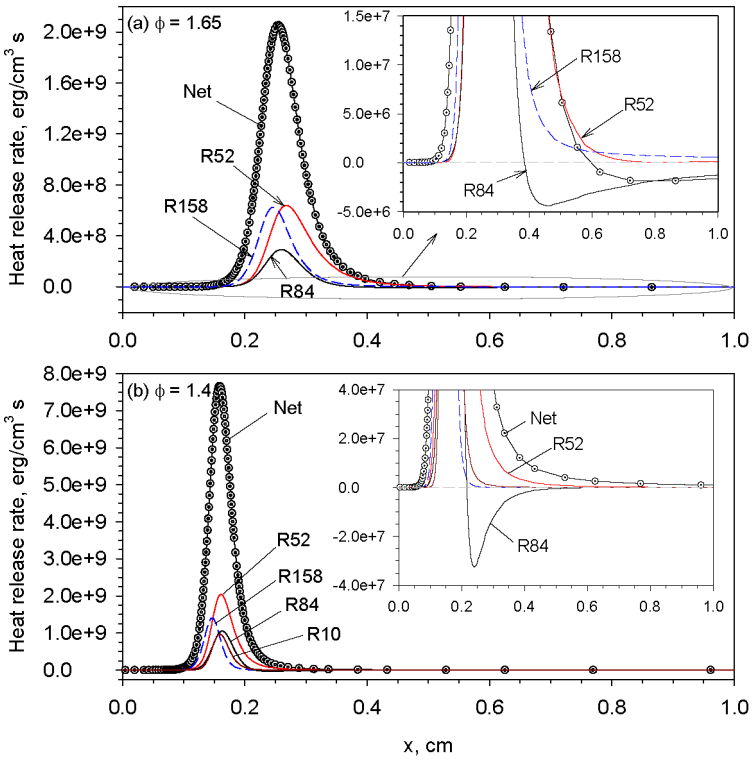

Fig. 13. Spatial distributions of major heat release reactions in two CH_4/air flames of $\phi = 1.65$ and 1.4.

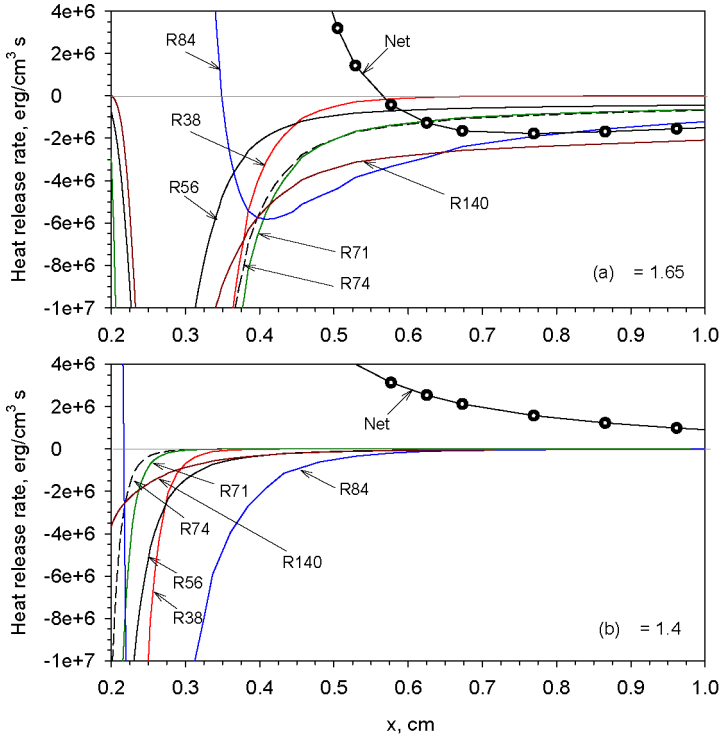

Fig. 14. Major endothermic reactions at the end of the reaction zones in two CH_4/air flames of $\phi = 1.65$ and 1.4.

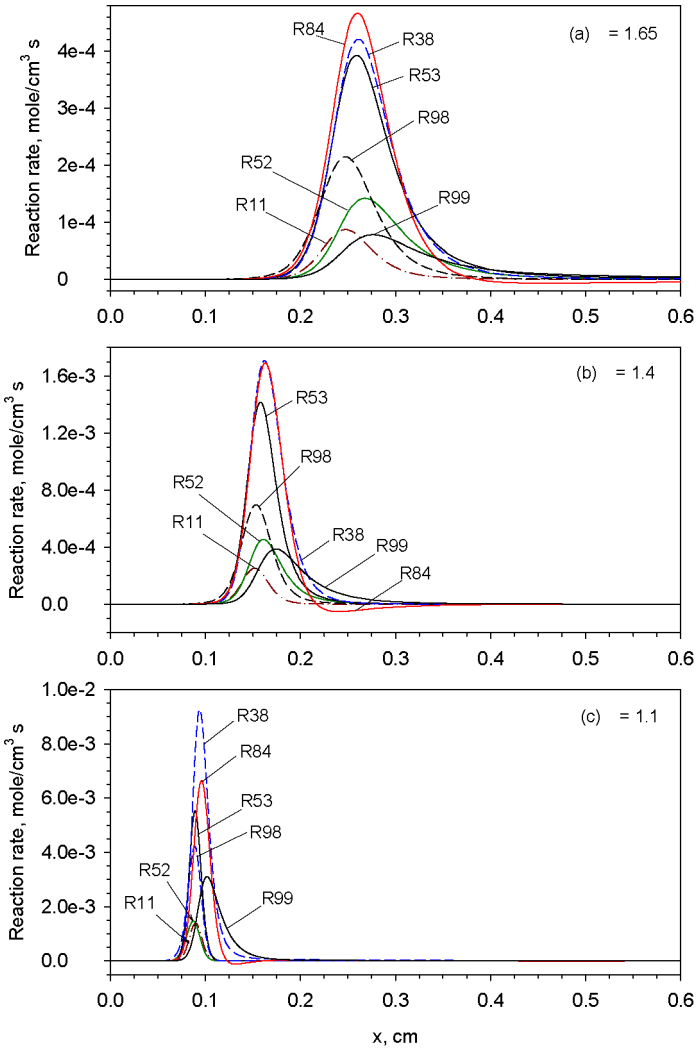

Fig. 15. Comparison of reaction rates of fuel consumption reactions $OH + H_2 \Leftrightarrow H_2O + H$ (R84), $H + O_2 \Leftrightarrow O + OH$ (R38), and $CO + OH \Leftrightarrow CO_2 + H$ (R99) in CH_4/air flames of $\phi = 1.65$, 1.4, and 1.1.

via R140, the H radical is involved in all other reactions. To examine how these reactions behave in a less richer flame, the heat release rates of these reactions for the $\phi = 1.4$ flame are shown in Fig. 14b. It is evident that these reactions reach equilibrium much more rapidly in the $\phi = 1.4$ flame, approximately at about $x = 0.6$ cm, than in the $\phi = 1.65$ flame.

To further illustrate the effect of equivalence ratio on the relative importance of different reactions controlling fuel (CH_4) consumption, H radical, H_2, and H_2O concentrations, reaction rates of most relevant reactions in flames of $\phi = 1.65$, 1.4, and 1.1 are compared in Fig. 15. Also plotted in this figure are the reaction rates of $OH + CO \Leftrightarrow CO_2 + H$ (R99). The first observation is that the reactions require a much longer time to reach equilibrium as the equivalence ratio increases. Methane is primarily attached by H and OH radicals through $H + CH_4 \Leftrightarrow CH_3 + H_2$ (R53) and $OH + CH_4 \Leftrightarrow CH_3 + H_2O$ (R98). The reaction rate of $O + CH_4 \Leftrightarrow CH_3 + OH$ (R11) is relatively slow compared to those of R53 and R98. Methane is actually formed through recombination of H and CH_3 via $H + CH_3 + (M) \Leftrightarrow CH_4 + (M)$ (R52), which is an important contributor to heat release (Fig. 13). In CH_4/air flames, H_2O is formed predominantly through $OH + H_2 \Leftrightarrow H_2O + H$ (R84) and R98. The effect of the equivalence ratio on the relative importance of these reactions can be observed. First, R84 becomes relatively faster compared to $H + O_2 \Leftrightarrow O + OH$ (R38) and R53. At $\phi = 1.1$, R84 is slower than R38 and R53 (in the preheat and most part of the reaction region). At $\phi = 1.4$, R84 is almost identical to R38 in the reaction zone and to R53 up to about $x = 0.152$ cm

(Fig. 15b). As ϕ further increases, R84 becomes faster than R38 and R53 in the reaction zone, but slower in the postflame region ($x > 0.31$ cm) (Fig. 15a). Secondly, reaction $CH_3 + H + (M) \Leftrightarrow CH_4 + (M)$ (R52) also becomes increasingly important as the equivalence ratio increases. Thirdly, relative to R84, R99 becomes relatively slower with increasing ϕ, implying that the degree of departure from equilibrium for this reaction becomes smaller. This is consistent with the results shown in Fig. 10 where both CO and CO_2 are closer to their equilibrium values at the end of the major heat release reactions than H_2 and H_2O. For equivalence ratios greater than 1.4, the enhanced reaction rate of R84 in the preheat and reaction zones leads to overshoot of H_2O. Meanwhile, the H radical becomes relatively scarce, though the H radical still stays above its equilibrium value in the reaction zone (Figs. 3 and 11), as a result of effective competition for H by CH_4 and CH_3 through R53 and R52 with R84. The above discussions highlight the important role played by H radicals in the postflame region as the reactions proceed to equilibrium. Another important factor in slowing down the approach of reactions to equilibrium in rich mixtures is the rapid drop in flame temperature with increasing the equivalence ratio (Fig. 1).

To verify the important role of the termination reaction R52 in the occurrence of SAFT, numerical calculations were conducted for the $\phi = 1.65$ flame with reduced the forward reaction rate constant of R52 and some selected results are shown in Fig. 16. Also shown in the figure legend is the temperature overshoot, $T_{max} - T_{eq}$. With decreasing the reaction rate constant of R52, the degree of overshoot of the H_2O mole fraction decreases, and so does the degree of temperature overshoot. Meanwhile, the flame thickness is also reduced as a result of enhanced combustion. This is caused by the overall increased fuel consumption rate as the recombination rate of H and CH_3 through R52 is suppressed, leading to a higher H radical concentration (Fig. 16b). Suppression of the forward reaction rate of R52 also leads to a lower mole fraction of CH_2CO (Fig. 16c), whose overshoot in the reaction zone is also responsible for SAFT as discussed earlier. Therefore, enhanced H radical concentration not only helps reduce the overshoot of H_2O concentration but also the overshoot of CH_2CO. Although OH radical concentration also increases with decreasing forward reaction rate of R52 (Fig. 16d), the increase in OH radical concentration is less significant than that in H radical. That is why the reverse reaction of R84 benefits more than its forward reaction when the forward reaction rate of R52 is reduced. It should be pointed out that further reduction in the reaction rate constant of R52 alone cannot further lower the degree of temperature overshoot. As shown in Fig. 15a, reaction R38 also competes strongly with R84 (its reverse reaction) for H radicals. Numerical calculation was also conducted with a reduced forward reaction rate of R38 by a factor of 5 while reducing the forward reaction rate of R52 by a factor of 10,000. The results are also compared in Fig. 16. It is seen that the temperature overshoot is further reduced to only about 5 K, which is accompanied by further reduced overshoot of H_2O and CH_2CO mole fractions. It is quite possible that a further reduction in the forward reaction rate of R38 (while reducing the forward reaction rate of R52) can completely suppress the occurrence of SAFT. A reduction in the reaction rate of R38 drastically lowers the combustion intensity (the reaction zone becomes much wider), which is expected due to its vital chain-branching role in hydrocarbon combustion. Nevertheless, results shown in Fig. 16 support the above finding that the relative scarcity of H radicals in the reaction zone due to reactions with hydrocarbon species, such as CH_4 (R53), CH_3 (R52), and O_2 (R38), is responsible for the overshoot of H_2O and CH_2CO concentrations and the occurrence of SAFT.

The chemical kinetics responsible for the occurrence of SAFT in CH_4/O_2 flames was then examined. A reaction flux analysis conducted in the $\phi = 1.3$ CH_4/O_2 flame reveals that the following endothermic reactions take place in the postflame region, in order of decreasing importance:

$$H + OH + M \Leftrightarrow H_2O + M, \quad \text{(R43)}$$

$$OH + HO_2 \Leftrightarrow O_2 + H_2O, \quad \text{(R181)}$$

$$OH + H_2O_2 \Leftrightarrow HO_2 + H_2O, \quad \text{(R89)}$$

$$OH + H_2 \Leftrightarrow H + H_2O. \quad \text{(R84)}$$

It is therefore clear that the cause of endothermicity in the postflame region in this rich CH_4/O_2 flame is attributed to dissociation of H_2O only, though the primary pathways are now R43 and R181, instead of R84. To examine the pathways for H_2O production in this flame, the major relevant reactions are shown in Fig. 17. Although the two most important reactions for H_2O production are still R84 and R98, as in rich CH_4/air flames, reactions $OH + CH_4 \Leftrightarrow CH_2(S) + H_2O$ (R97), $OH + CH_3 \Leftrightarrow CH_2 + H_2O$ (R96), and $OH + CH_2O \Leftrightarrow HCO + H_2O$ (R101) also contribute considerably to H_2O formation. In rich CH_4/O_2 flames, H_2O is primarily destroyed by O radical in the reaction zone via $OH + OH \Leftrightarrow O + H_2O$ (R86). Reaction rates of the major fuel consumption pathways along with those of R84 and R38 are compared in Fig. 18. The relative importance of these reactions in rich CH_4/O_2 flames is very different from that in rich CH_4/air flame shown in Figs. 15a

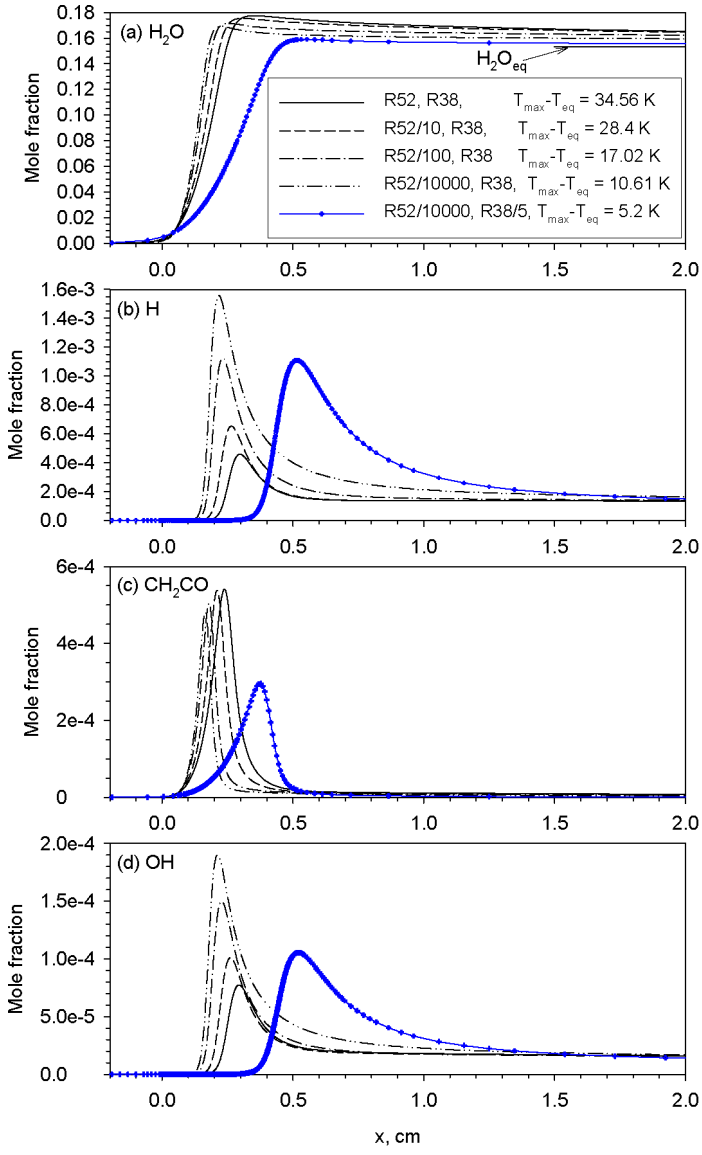

Fig. 16. Effects of the forward reaction rates of $CH_3 + H + (M) \Leftrightarrow CH_4 + (M)$ (R52) and $H + O_2 \Leftrightarrow O + OH$ (R38) on the spatial distributions of H_2O, H, CH_2CO, and OH in the CH_4/air flame of $\phi = 1.65$.

and 15b. In CH_4/air flames, the H radical is consumed not only by O_2 through R38 but also rapidly by CH_4 (through R53) and CH_3 (through R52). In CH_4/O_2 flames, however, both R53 and R52 reach equilibrium much more rapidly than R84 and R38. In other words, the structure of rich CH_4/O_2 flames exhibits two reaction zones: the hydrocarbon one located at roughly $x = 0.059$ cm where reaction rates of R53 and R98 peak, and the hydrogen one located slightly downstream at about $x = 0.062$ cm where reactions rate of R38 and R84 reach their maxima. This two reaction-zone structure of rich CH_4/O_2 flames indicates that the reactions in the postflame region are governed by the hydrogen chemistry. Fig. 18 shows that R38 is faster than R84 everywhere in the entire reaction zone, which is due to much higher flame temperatures and the abundance in O_2; see Fig. 4, for example. It is therefore plausible to assume that the overshoot of H_2O in rich CH_4/O_2 flames is a direct consequence of the scarcity of H radical; i.e., the rapid consumption of H radicals by R38 leads to overproduction of H_2O through forward reaction of R84 (while R98 also contributes substantially to the production of H_2O).

The validity of this assumption can be easily verified numerically by computing the $\phi = 1.3$ CH_4/O_2

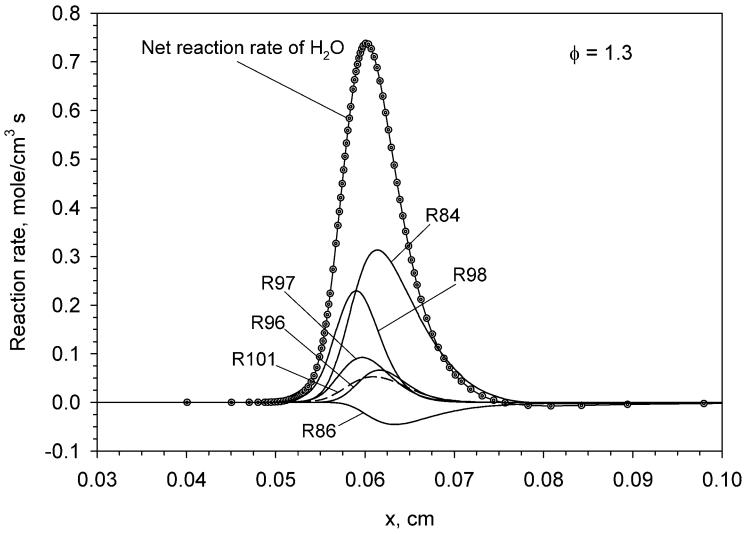

Fig. 17. Spatial distributions of rate of major reactions for the formation and destruction of H_2O in the CH_4/O_2 flame of $\phi = 1.3$.

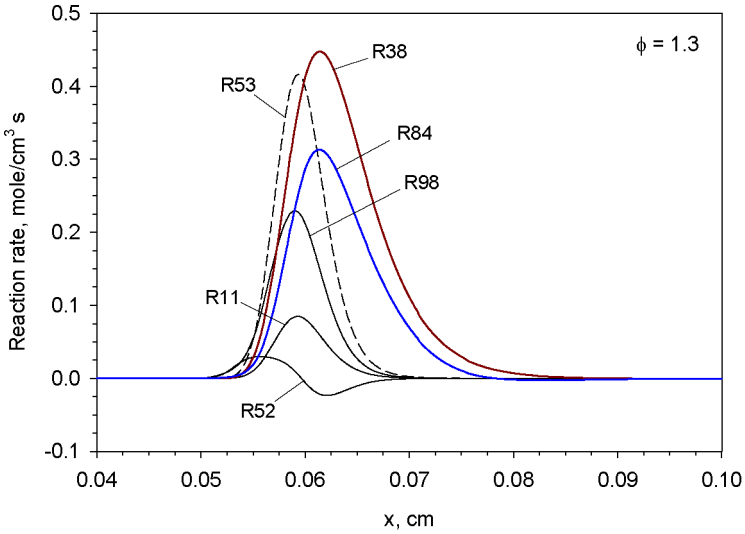

Fig. 18. Spatial distributions of rate of fuel consumption reactions $OH + H_2 \Leftrightarrow H_2O + H$ (R84), and $H + O_2 \Leftrightarrow O + OH$ (R38) in the CH_4/O_2 flame of $\phi = 1.3$.

flame with a reduced forward reaction rate constant of R38. The results with and without reduction (by a factor of 10) in the forward reaction rate constant of R38 are compared in Fig. 19. It is evident that SAFT phenomenon disappears when the reaction rate of R38 is reduced by a factor of 10 (Fig. 19a), which is directly related to the elimination of H_2O overshoot (Fig. 19b). The complete suppression of temperature and H_2O overshoot is indeed accompanied with enhanced, actually somewhat overshoot, H radical concentration in the immediate postflame region, as presumed above. A reduced reaction rate of R38 also leads to a lowered OH radical concentration, which also helps suppress H_2O formation by reducing the forward reaction rate of R84. Results shown in Fig. 19 once again confirm that the nature of SAFT in rich CH_4/O_2 flames is also the scarcity of H radicals, as in rich CH_4/air flames.

The above discussions lead to the conclusion that the nature of SAFT in rich CH_4 flames is the relative scarcity of H radicals. Although the reaction pathways responsible for the shortage of H radicals in CH_4/air and CH_4/O_2 flames are somewhat different, they share the same chemical nature. Insight into the important role of H radicals gained above also helps in understanding the very different influence of H radical preferential diffusion in CH_4/air and CH_4/O_2 flames.

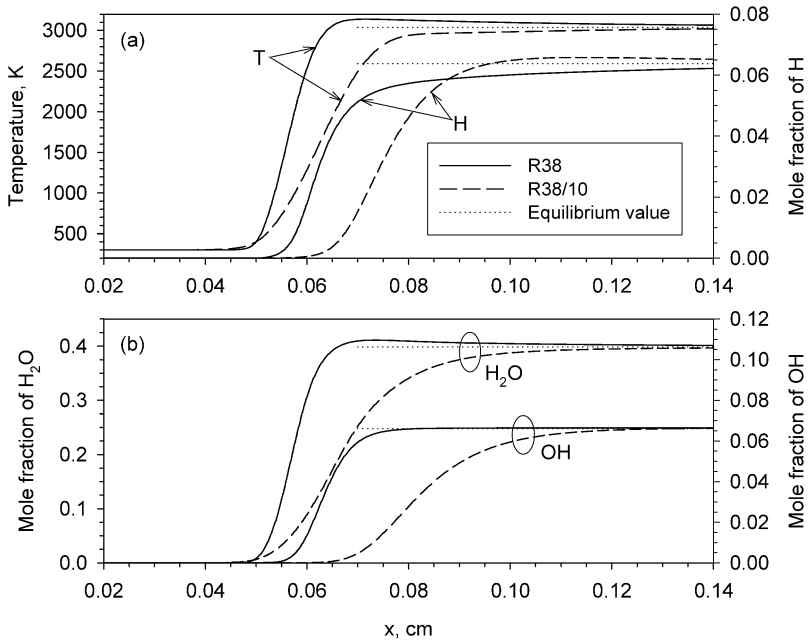

Fig. 19. Effect of the forward reaction rate of $H + O_2 \Leftrightarrow O + OH$ (R38) on the spatial distributions of T, H, H_2O, and OH in the CH_4/O_2 flame of $\phi = 1.3$.

4. Conclusions

A systematical numerical study of the effects of the preferential diffusion of H_2 and H from the reaction zone to the preheat zone and the unity Lewis number for all species on the phenomenon of superadiabatic flame temperature was conducted in rich CH_4/air and CH_4/O_2 mixtures using detailed chemistry. These objectives were achieved by employing five different species diffusion models in the calculations. The numerical results demonstrate that the preferential diffusion of H_2 and H from the reaction zone to the preheat zone and the unity Lewis number have only a very small influence on the maximum flame temperatures in rich CH_4/air mixtures. In rich CH_4/O_2 mixtures, the elimination of the preferential diffusion of H_2 alone not only does not reduce the maximum flame temperature, but actually slightly increases it. The suppression of the preferential diffusion of the H radical from the reaction zone to the preheat zone completely eliminates the occurrence of superadiabatic flame temperature for equivalence ratios between 0.9 and 1.15 and drastically reduces the degree of superadiabaticity for richer mixtures in CH_4/O_2 flames. Compared to the results of suppressing the preferential diffusion of the H radical alone, the assumption of unity Lewis number for all species results in further reduction in overall combustion intensity due to the chemically inhibiting effect of CO_2 diffused from the postflame region to the reaction zone.

Through reaction flux analyses, it was revealed that the fundamental cause of superadiabatic flame temperature in rich CH_4/air and CH_4/O_2 flames is the relative scarcity of H radicals at the end of major heat release reactions. However, the chemical pathways for the shortage of H radicals in these two types of flame are somewhat different. In CH_4/air flames, the scarcity of H radicals is a result of competition from hydrocarbon species, such as CH_4 and CH_3 through $H + CH_4 \Leftrightarrow CH_3 + H_2$ and $H + CH_3 + (M) \Leftrightarrow CH_4 + (M)$, and O_2 through $H + O_2 \Leftrightarrow O + OH$. In CH_4/O_2 flames; however, the shortage of the H radical is caused by O_2 through $H + O_2 \Leftrightarrow O + OH$ due to its abundance and high flame temperatures. The present investigation along with numerical experiments confirm that the nature of the superadiabatic flame temperature phenomenon in rich methane premixed flames is not the preferential diffusion of H_2 from the reaction zone to the preheat zone, but the relative shortage of H radicals in the immediate postflame region. It is anticipated that any chemical processes, such as chemically active additives, or physical processes, such as preheat or preferential diffusion, that can alter the H radical concentration in the reaction zone, will directly affect the occurrence of superadiabatic flame temperature; reduction in the H radical in the reaction zone prompts temperature overshoot, while enhancement in the H radical in the reaction zone suppresses temperature overshoot. The high diffusivity of H rad-

icals, due to its small molecular weight, produces significant losses of H radicals out of the reaction zone of the flame, contributing to the SAFT phenomenon that has been reported for rich hydrocarbon flames.

References

[1] E. Meeks, R.J. Kee, D.S. Dandy, M.E. Coltrin, Combust. Flame 92 (1993) 144.
[2] K.E. Bertagnolli, R.P. Lucht, Proc. Combust. Inst. 26 (1996) 1825.
[3] K.E. Bertagnolli, R.P. Lucht, M.N. Bui-Pham, J. Appl. Phys. 83 (1998) 2315.
[4] B. Ruf, F. Behrendt, O. Deutschmann, S. Kleditzsch, J. Warnatz, Proc. Combust. Inst. 28 (2000) 1455.
[5] F. Liu, H. Guo, G.J. Smallwood, Ö.L. Gülder, Proc. Combust. Inst. 29 (2002) 1543.
[6] V.V. Zamashchikov, I.G. Namyatov, V.A. Bunev, V.S. Babkin, Combust. Explosion Shock Waves 40 (2004) 32.
[7] T. Takagi, Z. Xu, Combust. Flame 96 (1994) 50.
[8] R.J. Kee, J.F. Grcar, M.D. Smooke, J.A. Miller, Sandia Report SAND 85-8240, 1985.
[9] R.J. Kee, J.A. Miller, T.H. Jefferson, Sandia Report SAND 80-8003, 1980.
[10] J. Warnatz, R.J. Kee, J.A. Miller, Sandia Report SAND 83-8209, 1983.
[11] G.P. Smith, D.M. Golden, M. Frenklach, N.W. Moriarty, B. Eiteneer, M. Goldenberg, C.T. Bowman, R.K. Hanson, S. Song, W.C. Gardiner Jr., V.V. Lissianski, Z. Qin, http://www.me.berkeley.edu/gri_mech/.
[12] F. Liu, H. Guo, G.J. Smallwood, Combust. Flame 133 (2003) 495.